Hydrostatic-pressure determination of tensile-strained $Ga_xIn_{1-x}P$-$(Al_yGa_{1-y})_{0.52}In_{0.48}P$ quantum-well band offsets

O. P. Kowalski, J. W. Cockburn, D. J. Mowbray, and M. S. Skolnick
Department of Physics, University of Sheffield, Sheffield S3 7RH United Kingdom

M. D. Dawson, G. Duggan, and A. H. Kean
Sharp Laboratories of Europe Ltd., Edmund Halley Road, Oxford Science Park, Oxford OX4 4GA United Kingdom
(Received 20 October 1995; revised manuscript received 27 December 1995)

Photoluminescence, measured as a function of hydrostatic pressure, has been used to determine the band offsets of two tensile-strained $Ga_xIn_{1-x}P$-$(Al_yGa_{1-y})_{0.52}In_{0.48}P$ quantum-well structures. Unlike other techniques commonly used to determine band offsets, this method has the advantage that a detailed knowledge of the material parameters is not required. Conduction-band offsets of $\Delta E_c=(0.79\pm0.07)\Delta E_G^{\mathrm{HH}}$ and $\Delta E_c=(0.74\pm0.10)\Delta E_G^{\mathrm{HH}}$, where ΔE_G^{HH} is the total heavy-hole-related band-gap discontinuity, are obtained for structures having strains of $+0.56$ and $+0.71\%$ and barrier Al compositions of 0.7 and 0.55, respectively. Alternatively the band offsets expressed in terms of the light-hole band-gap discontinuity are ΔE_c: $\Delta E_G^{\mathrm{LH}}=0.70{:}0.30$ and 0.61:0.39 [corresponding to absolute light-hole valence-band offsets of $\Delta E_V^{\mathrm{LH}}=(110\pm12)$ meV and (113 ± 15) meV] for the $+0.56$ and $+0.71\%$ strained samples, respectively. At high pressures the structures become type II, and the observed indirect real and k-space transition exhibits a blueshift with increasing incident laser power density. An analysis of this blueshift allows both the density and lifetime of the spatially separated photoexcited carriers to be determined.

I. INTRODUCTION

$Ga_xIn_{1-x}P$-$(Al_yGa_{1-y})_{0.52}In_{0.48}P$ heterostructures, with $x=0.52$, represent the largest direct band gap, III-V GaAs-lattice-matched low-dimensional semiconductor system. They hence possess considerable potential for efficient, visible electro-optical applications including ultrabright red-green light-emitting diodes,[1] and both conventional geometry[2] and vertical cavity surface-emitting[3] visible laser diodes. By altering the Ga:In ratio of the $Ga_xIn_{1-x}P$ well material, the active region of $Ga_xIn_{1-x}P$-$(Al_yGa_{1-y})_{0.52}In_{0.48}P$ heterostructures may be subjected to either tensile ($x>0.52$) or compressive ($x<0.52$) strain. Both types of strain have been predicted[4,5] to lead to improved laser diode performance, compared to unstrained devices, due to strain modifications of the valence-band structure. Tensile strain is expected to reduce spontaneous emission losses in the plane of the layers, and there is some experimental evidence to suggest that $Ga_xIn_{1-x}P$-$(Al_yGa_{1-y})_{0.52}In_{0.48}P$ devices with tensile-strained active layers exhibit reduced threshold current densities.[6]

In order to accurately model and optimize device behavior, a reliable knowledge of the heterojunction band offsets is required. Although there have been a number of reports of measurements of unstrained $Ga_xIn_{1-x}P$-Al(Ga)InP band offsets,[7–13] and, to a more limited extent, for compressively strained structures,[13–15] very little is known about the band offsets of the tensile-strained $Ga_xIn_{1-x}P$-$(Al_yGa_{1-y})_{0.52}In_{0.48}P$ system. To the best of our knowledge there has been only one reported determination of such offsets[16] where an optical technique, applied to samples with a strain of $+0.56\%$ ($x=0.59$), gave a conduction band offset $\Delta E_c\sim0.7\Delta E_G^{\mathrm{HH}}$,[16] ΔE_G^{HH} being the total heavy-hole band-gap discontinuity.

In the present paper we describe the use of hydrostatic pressure to directly determine the band offsets of tensile strained $Ga_xIn_{1-x}P$-$(Al_yGa_{1-y})_{0.52}In_{0.48}P$ quantum wells. This technique, in which the low-temperature photoluminescence is measured as a function of hydrostatic pressure,[7,8,11–13,17] provides a direct and reliable determination of the band offsets. Unlike other techniques which are commonly used to determine heterojunction band offsets, it requires a knowledge of relatively few material parameters. Such parameters are often not well known for ternary- and quaternary-containing heterojunction systems, and this limits the accuracy and reliability of many of the more commonly employed methods used to determine band offsets.

II. SAMPLE AND EXPERIMENTAL DETAILS

Two tensile-strained $Ga_xIn_{1-x}P$-$(Al_yGa_{1-y})_{0.52}In_{0.48}P$ quantum-well structures have been studied. The first, which is grown by metal-organic vapor-phase epitaxy (MOVPE), has $(x,y)=(0.59,0.7)$ and consists of a 300-Å single quantum well (SQW) confined between 0.1- and 1-μm barrier layers. The composition of the well results in it being subjected to an in-plane tensile strain of $+0.56\%$. Growth conditions for this sample are designed to minimize the effects of the spontaneous ordering which can occur in MOVPE-grown $Ga_xIn_{1-x}P$ and $(Al_yGa_{1-y})_{0.52}In_{0.48}P$.[18] Full details of the growth and characterization of this and related samples are given in Ref. 16. The second sample is grown by gas-source molecular-beam epitaxy (GS-MBE), and consists of a seven-period multiple quantum well (MQW) with $(x,y)=(0.61,0.55)$ and 55-Å wells and 37-Å barriers. This well composition produces an in-plane tensile strain of $+0.71\%$. The quantum-well stack is confined between 0.1-

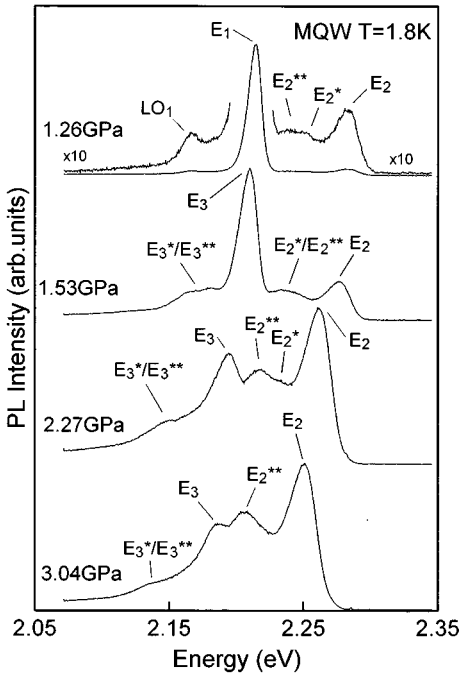

FIG. 1. Typical PL spectra of the MQW sample recorded for various values of applied hydrostatic pressure at 1.8 K.

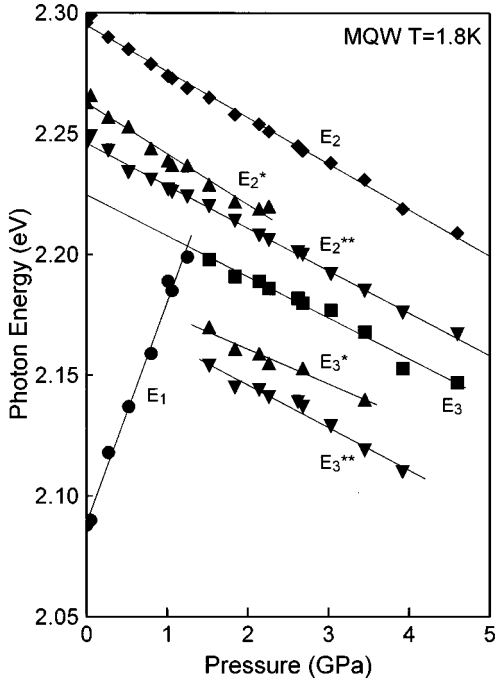

FIG. 2. PL measured transition energies of the MQW plotted against applied hydrostatic pressure.

and 1.0-μm-thick $Al_xGa_{1-x}InP$ layers of a composition equal to that of the barriers. Growth is on a (001) GaAs substrate misoriented by 15° toward (111)*A* again to minimize possible ordering effects. The barriers of both samples are nominally unstrained.

Hydrostatic pressure was applied to the samples at 1.8 K in a miniature diamond-anvil cell.[19] The samples were mechanically thinned to a thickness of ~ 50 μm and then cleaved to a size $\sim 100 \times 100$ μm^2 before mounting in the cell. A ruby chip was used as a pressure sensor with argon as a pressure transmitting medium. The photoluminescence (PL) was excited with the 4765-Å line of an Ar-ion laser, using incident power densities in the range $\sim 2-30$ W cm^{-2}, and was detected with a triple spectrometer and a multichannel charge coupled device (CCD) system.

III. EXPERIMENTAL RESULTS

A. MQW sample

Figure 1 shows typical PL spectra of the MQW, recorded for a number of pressures. At low pressures the dominant PL (E_1) arises from recombination between the lowest well electron and the highest well valence-band states. Both these states are at $k=0$ (Γ). Hence transition E_1 is direct in both real and k space. Because the well is subjected to tensile strain, the lowest-energy valence-band state is the first light-hole level (LH1). Without the effects of quantum confinement, and a well composition of $x=0.61$, this state lies 52 meV lower in energy than the first heavy-hole state (HH1). Although confinement effects reduce this splitting, we calculate that, for the 55-Å well width of the present sample, LH1 lies 18 meV below HH1. The higher-energy, weaker features in the PL spectra arise from recombination in the barriers. This consists of a main peak (E_2) and weaker impurity- or defect-related peaks (E_2^* and E_2^{**}). Also observed in the low-pressure spectra is the first LO-phonon satellite (LO_1) of transition E_1. This feature, which corresponds to E_1 recombination and the additional emission of a longitudinal-optical phonon, has been discussed elsewhere,[9,20] and will not be considered further in this paper. In Fig. 2 the measured PL transition energies of the MQW are plotted against pressure. For clarity the phonon satellite associated with the E_1 transition is omitted. With increasing pressure the E_1 quantum-well transition shifts to higher energy at a rate (91.7 ± 0.35) meV/GPa, consistent with the behavior expected for a transition between zone-center electron and hole states ($\Gamma \rightarrow \Gamma$). In contrast, the barrier transition E_2 exhibits a smaller and negative pressure coefficient of (-19.1 ± 0.3) meV/GPa, typical of transitions between electron states at the $k \neq 0$ X point and hole states at the zone center ($X \rightarrow \Gamma$). This behavior is in agreement with studies of bulk $(Al_xGa_{1-x})_{0.52}In_{0.48}P$, which show that for $x \gtrsim 0.52$ the material has an indirect band gap.[21,22] For pressures above ≈ 1.3 GPa the E_1 transition disappears, and a series of transitions (E_3, E_3^*, and E_3^{**}) appear, all of which exhibit a small, negative pressure coefficient [(-17.0 ± 0.9) meV/GPa for E_3].

The negative pressure coefficient of the E_3 transition indicates that, like E_2, it originates from an X state. For this there are two possibilities, either the well X state (X_W) or the barrier X state (X_B). In both cases the final hole state will be in the well (Γ_W) as this represents the highest valence-band state for all pressures. Both possibilities for E_3 ($X_W \rightarrow \Gamma_W$ and $X_B \rightarrow \Gamma_W$) are indicated in Fig. 3, which is a schematic band diagram of the sample at ambient pressure. Details of the calculations of the energy levels shown in Fig. 3 will be described below. At ambient pressure recombination associated with $X_W \rightarrow \Gamma_W$ will not be observed due to the zero-

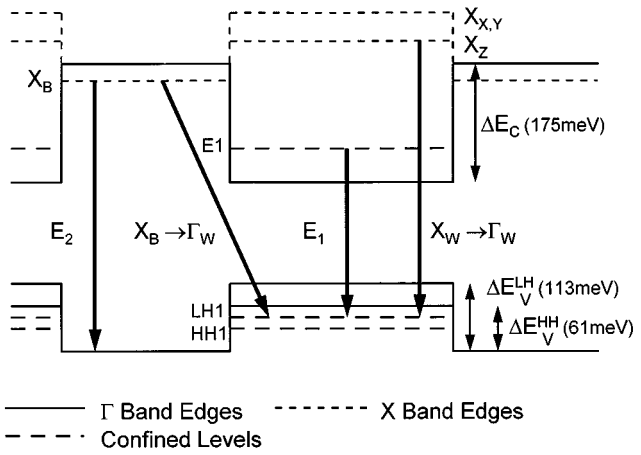

FIG. 3. Schematic band diagram of the MQW at ambient pressure. For clarity the energy axis is not drawn to scale.

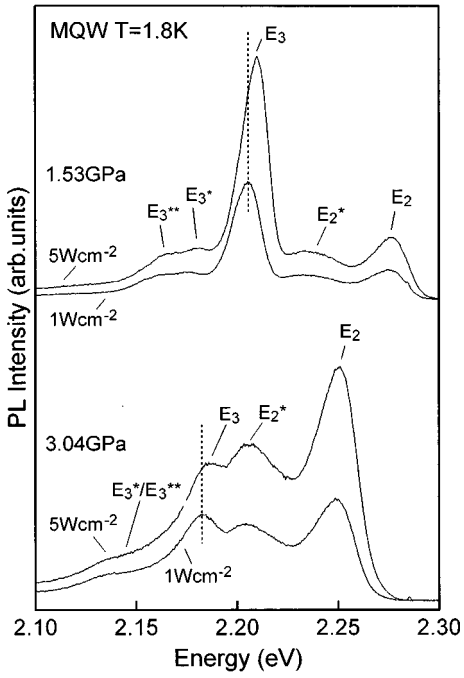

FIG. 4. The incident laser power density dependence of the PL spectra of the MQW. Spectra are shown recorded for incident power densities of 1 and 5 W cm^{-2} at pressures of 1.53 and 3.04 GPa.

electron population of X_W. In addition, the $X_B \rightarrow \Gamma_W$ transition is unlikely to be visible due to the low population of X_B and the small wave-function overlap between the spatially separated states X_B and Γ_W. However, with increasing hydrostatic pressure the X states move down and the Γ electron states move up in energy. Hence, above a certain pressure the lowest X state will become the lowest electron state. Its population will increase, and transitions from this state will be observed.

Inspection of Fig. 3 shows that the relative positions of X_W and X_B depend not only on the magnitude of the well and barrier indirect band gaps but also on the size of the valence-band offset. Furthermore, the valence-band offset for the light-hole states, ΔE_V^{LH}, is given by

$$\Delta E_V^{\mathrm{LH}} \approx E_2 - E(X_B \rightarrow \Gamma_W) + E_{\mathrm{LH1}}, \tag{1}$$

where $E(X_B \rightarrow \Gamma_W)$ is the energy of the $X_B \rightarrow \Gamma_W$ transition, and E_{LH1} is the confinement energy of the first light-hole state. Hence, if the experimentally observed transition E_3 is due to $X_B \rightarrow \Gamma_W$ because X_B is the lowest X state, then, by extrapolating its energy back to ambient pressure, the valence-band offset can be determined from a knowledge of E_2 and E_{LH1}. However, if E_3 is due to $X_W \rightarrow \Gamma_W$ because X_W is the lowest X state, then only a lower limit can be placed on the size of $E(X_B \rightarrow \Gamma_W)$ and hence on ΔE_V^{LH}.

In order to determine whether E_3 is due to $X_W \rightarrow \Gamma_W$ or $X_B \rightarrow \Gamma_W$, PL spectra were recorded as a function of the incident laser power density. Typical spectra, recorded for power densities of ~ 1 and 5 W cm^{-2}, at pressures of 1.53 and 3.04 GPa, are shown in Fig. 4. At both pressures, increasing the incident laser power density causes the E_3 transition to blueshift to higher energy by ≈ 4 meV. In contrast, the barrier transition E_2 exhibits no power-dependent blueshift within the experimental accuracy. In addition, the intensity of E_3 becomes weaker relative to that of E_2 as the power density is increased. The power-dependent blueshift of E_3 can be understood if this transition occurs between spatially separated initial and final states (i.e., $X_B \rightarrow \Gamma_W$).[23,24] The net negative charge due to electrons in the barriers produces an electrostatic band bending of an opposite sign to that produced by the net positive charge of holes in the well. The energies of both the initial electron and final hole states of a spatially indirect transition are hence increased, resulting in an overall increase, with increasing carrier density, of the transition energy. In addition, the small overlap between the wave functions of the initial and final states results in a long recombination time. A large charge buildup, and hence large band bending and resultant blueshift, therefore occurs for moderate incident laser powers. In contrast, transitions between nonspatially separated states (i.e., $X_W \rightarrow \Gamma_W$) will be unaffected by any space-charge-induced band bending as, to a first approximation, the effect on electron and hole states in the same layer will be equal and of the same sign.[23] The overall effect on the energy of a spatially direct transition will therefore be zero. The reason for the variation of the relative intensities of E_2 and E_3 as the incident laser power density is increased is unclear. However, we have observed a similar behavior in unstrained $Ga_{0.52}In_{0.48}P$-$(Al_yGa_{1-y})_{0.52}In_{0.48}P$ MQWs where the E_3 transition could be unambiguously assigned to $X_B \rightarrow \Gamma_W$ both from its observed blueshift with increasing laser power density and the variation of its energy between samples of different barrier Al composition.[7,8]

From the observed behavior of E_3, we therefore conclude that it is the $X_B \rightarrow \Gamma_W$ indirect real and k-space transition with E_3^* and E_3^{**} resulting from defect/impurity states associated with X_B and/or Γ_W. This result implies that X_B lies below X_W in the present sample. Having identified E_3 as being due to $X_B \rightarrow \Gamma_W$, the band offsets of the sample can now be determined. Equation (1) can be rewritten as

$$\Delta E_V^{\mathrm{LH}} = E_2^g - E_3^g + E_{\mathrm{LH1}}, \tag{2}$$

where E_2^g and E_3^g are the zero-pressure, free-particle band gaps corresponding to transitions E_2 and E_3, respectively. As we have discussed in a previous publication,[7] in order to relate the free-particle band gaps to the experimentally determined transition energies, corrections for both excitonic and localization effects must be applied. Accounting for these, Eq. (2) becomes

$$\Delta E_V^{\mathrm{LH}} = (E_{2,m}^0 - E_{3,m}^0) + (E_{2,\mathrm{ex}} - E_{3,\mathrm{ex}}) + (E_{2,\mathrm{loc}} - E_{3,\mathrm{loc}}) + E_{\mathrm{LH1}}, \quad (3)$$

where $E_{i,m}^0$, $E_{i,\mathrm{ex}}$, and $E_{i,\mathrm{loc}}$ are the measured zero-pressure transition energy, exciton binding energy, and localization energy, respectively, of the ith transition. $E_{2,m}^0$, the zero-pressure barrier indirect band-gap transition energy, is obtained from the zero-pressure spectra, and the zero-pressure value of the spatially indirect transition $E_{3,m}^0$ is obtained by extrapolating back to zero pressure the transitions plotted in Fig. 2. The value of the latter is adjusted slightly to correct for the blueshift induced by the incident laser power density used to obtain the data of Fig. 2. For the barrier indirect band-gap exciton binding energy $E_{2,\mathrm{ex}}$, we assumed a value of 20 meV, equal to the experimentally measured value for GaP.[25] $E_{3,\mathrm{ex}}$ is the exciton binding energy of the indirect real and k-space transition $X_B \rightarrow \Gamma_W$. Because of the spatial separation of the electron and hole, this will have a value less than that of a corresponding bulk three-dimensional (3D) exciton. For the layer thicknesses of the present sample calculations by Duggan and Ralph,[26] for the case of a type-II GaAs-AlAs superlattice, indicate an indirect exciton binding energy of approximately half the bulk AlAs value. Although the effective masses of the GaAs-AlAs and $Ga_xIn_{1-x}P$-$(Al_yGa_{1-y})_{0.52}In_{0.48}P$ systems are similar, the band offsets of the former system are considerably greater. This latter difference will lead to a larger indirect exciton binding energy for the $Ga_xIn_{1-x}P$-$(Al_yGa_{1-y})_{0.52}In_{0.48}P$ system due to the greater penetration of the electron and hole wave functions into their respective barriers which will reduce their effective spatial separation. We therefore assume a value for $E_{3,\mathrm{ex}}$ of half the bulk GaP value, although from the above discussion this may slightly underestimate its true value. The penultimate term in Eq. (3) represents the difference between the localization energies for the two transitions E_2 and E_3. PL and PLE measurements of high Al content $(Al_xGa_{1-x})_{0.52}In_{0.48}P$ layers give a localization energy of $\sim$30 meV for recombination at the indirect band gap.[21,22] The difference between the two localization energies is difficult to calculate but, given that they both have the same initial state, a reasonable approximation is to assume that they are equal to within 10 meV and hence that $E_{2,\mathrm{loc}} - E_{3,\mathrm{loc}} = (0 \pm 10)$ meV.

Using Eq. (3), the valence-band offset for light holes can now be determined. The only additional parameter required is E_{LH1}, for which a value of 30 meV is calculated using a finite depth square-well model which includes the effects of coupling between the light and spin-orbit split-off bands. With this value for E_{LH1}, Eq. (3) gives $\Delta E_V^{\mathrm{LH}} = (113 \pm 15)$ meV. The errors in this value are due to uncertainties in the zero-pressure intercepts of E_2 and E_3 determined from Fig. 2, and errors in the calculated terms in Eq. (3). Having determined ΔE_V^{LH}, the conduction band offset ΔE_c can be calculated if the well and barrier direct band gaps are known. The barrier band gap is measured directly by photoluminescence excitation (PLE), and a value of (2.357 ± 0.010) eV is obtained after correction for the exciton binding energy. For the strained well a light-hole-related bulk band gap of (2.069 ± 0.015) eV is calculated using Eq. (1) of Ref. 16 for the unstrained band gap of $Ga_xIn_{1-x}P$, the theory of Ref. 27 for the effects of strain on the direct band gap, and material parameters given in Ref. 16. From these values a conduction-band offset of (175 ± 23) meV is determined and, using a calculated value of (2.121 ± 0.010) eV for the well heavy-hole band gap, a heavy-hole offset $\Delta E_V^{\mathrm{HH}} = (61 \pm 25)$ meV is deduced. Finally, expressing the conduction-band offset as a fraction of the total heavy-hole band gap discontinuity $(\Delta E_G^{\mathrm{HH}})$ gives the result $\Delta E_c = (0.74 \pm 0.10)\Delta E_G^{\mathrm{HH}}$. Alternatively expressing ΔE_c as a fraction of the total light-hole band-gap discontinuity $(\Delta E_G^{\mathrm{LH}})$ gives the result $\Delta E_c = (0.61 \pm 0.08)\Delta E_G^{\mathrm{LH}}$. These calculated values are indicated on the schematic band diagram of Fig. 3.

As discussed above, the relative position of the well and barrier X states (X_W and X_B) depends not only upon the sizes of the bulk indirect band gaps but also on the magnitude of the valence-band offset. In order to observe the indirect real and k-space transition $X_B \rightarrow \Gamma_W$, and hence to be able to determine the band offsets, X_B must lie below X_W. Reference to Fig. 3 shows that this requires

$$E_B^{\mathrm{IND}} < E_W^{\mathrm{IND}} + \Delta E_V^{\mathrm{LH}}, \quad (4)$$

where E_B^{IND} and E_W^{IND} are the barrier and well indirect bulk band gaps, the latter measured with respect to the strained light-hole valence-band edge. Confinement effects are neglected due to the large X-point effective masses. Measurements of bulk $(Al_xGa_{1-x})_{0.52}In_{0.48}P$ (Refs. 21 and 22) and $Ga_xIn_{1-x}P$ (Refs. 28 and 29) give values for E_B^{IND} and the indirect band gap of unstrained $Ga_{0.61}In_{0.39}P$ of 2.325 and 2.310 eV, respectively. The effect of tensile strain on the indirect band gap of $Ga_{0.61}In_{0.39}P$ has three components; a positive hydrostatic term, a negative term resulting from the strain splitting of the valence band, and a similar negative term for the X states which results in the X valley along the growth direction (X_z) forming the lowest quantum-well X state. To calculate the size of these effects, we use an indirect gap hydrostatic pressure deformation potential of $+1.52$ eV, derived from hydrostatic pressure measurements of GaAs lattice-matched $Ga_{0.52}In_{0.48}P$,[30] and the X-point shear deformation potential of GaP.[25] This calculation assumes, as do all the calculations in this paper, that the sample growth direction is (001). The errors introduced by the deviation of the actual growth directions away from (001) are expected to be small, and are certainly less than errors arising from the uncertainties in the precise values of the material parameters used in the calculations. The overall effect of the strain is to reduce the well indirect band gap by 77 meV, and the relative positions of the well X states are indicated in Fig. 3. With these values for E_B^{IND} and E_W^{IND}, Eq. (4) requires that $\Delta E_V^{\mathrm{LH}} > 92$ meV or, alternatively, $\Delta E_C < 196$ meV. Expressing ΔE_C as a fraction of the total heavy-hole band-gap discontinuity results in the inequality $\Delta E_C < 0.83\Delta E_G^{\mathrm{HH}}$. The

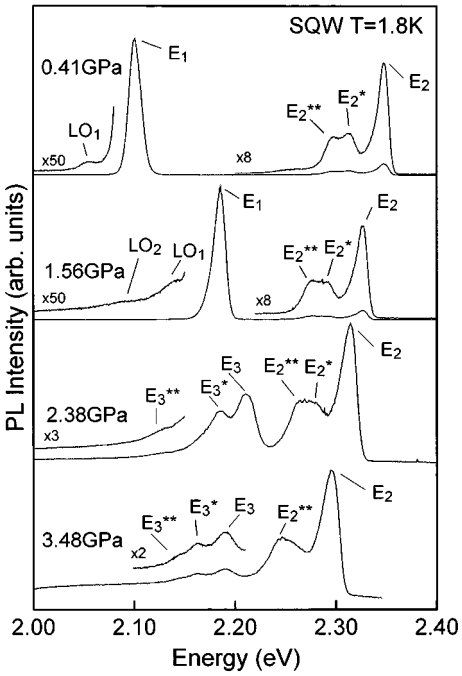

FIG. 5. Typical PL spectra of the SQW sample recorded for various values of applied hydrostatic pressure at 1.8 K.

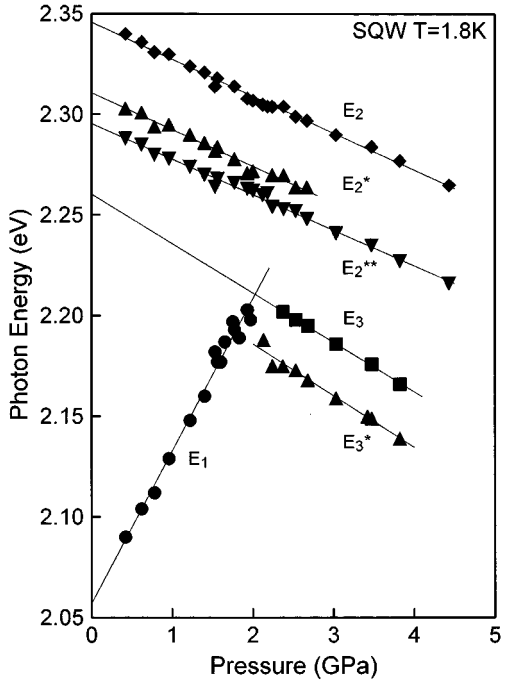

FIG. 6. PL measured transition energies of the SQW plotted against applied hydrostatic pressure.

value deduced above for ΔE_C is fairly close to but within this limit, providing further support for the above assignment of E_3 to the type-II indirect real and k-space transition $X_B \rightarrow \Gamma_W$.

B. SQW sample

Figure 5 shows PL spectra of the SQW recorded as a function of pressure. The form and behavior of these spectra are very similar to those of the MQW sample described above. The low-pressure spectra are again dominated by the direct quantum-well transition (E_1) with weaker barrier PL at higher energy (E_2, E_2^*, and E_2^{**}). The pressure coefficients of these transitions are (76 ± 1) meV/GPa and (-18.3 ± 0.8) meV/GPa, respectively. For pressures above $\approx$2.0 GPa, E_1 is quenched and is replaced by E_3 and related transitions all showing a negative pressure coefficient of (-25 ± 1) meV/GPa. The energies of the PL transitions for the SQW are plotted against pressure in Fig. 6. A reliable determination of the SQW band offsets again requires that the experimentally observed feature E_3 is due to the indirect real and k-space $X_B \rightarrow \Gamma_W$ transition. PL spectra recorded for different incident laser power densities show a small blueshift of E_3 with increasing power, although, in contrast to the MQW, E_3 becomes more intense in relation to the barrier transition E_2 as the laser power is increased.

The observed blueshift of E_3 and the result of calculations,[31] which indicate that if X_B is the lowest X state in the MQW then it must also be the lowest X state in the SQW, allows us to conclude that E_3 is due to the $X_B \rightarrow \Gamma_W$ transition. The light-hole-related valence-band offset can now be determined from Eq. (3). The only difference compared to the MQW is that, because of the wide well width of the SQW, the hole confinement energy (E_{LH1}) is very small ($\approx$2 meV), and the binding energy of the spatially indirect transition exciton ($E_{3,\mathrm{ex}}$) is essentially zero. The experimentally determined values then give $\Delta E_V^{\mathrm{LH}} = (110\pm12)$ meV. Using PLE-measured values for the well and barrier band gaps, values of $\Delta E_c = (260\pm19)$ meV and $\Delta E_V^{\mathrm{HH}} = (68\pm21)$ meV are determined for the conduction and heavy-hole-related band offsets, respectively. Finally, expressing the conduction-band offset as a fraction of the total heavy-hole band-gap discontinuity gives $\Delta E_c = (0.79\pm0.07)\Delta E_G^{\mathrm{HH}}$ or, as a fraction of the total light-hole band-gap discontinuity, $\Delta E_c = (0.70\pm0.07)\Delta E_G^{\mathrm{LH}}$. Calculations for this sample using Eq. (4) show that the observation of the type-II transition requires $\Delta E_c < 0.89\Delta E_G^{\mathrm{HH}}$, providing additional support for the validity of this band-offset determination.

It is interesting to note that there is some difference in the pressure coefficients of nominally identical transitions for the two samples. The reason for this behavior is unclear, but probably indicates the presence of nonhydrostatic pressure coefficients (i.e., biaxial strain) within the samples. This may be an intrinsic effect due to the different bulk moduli of the well, barrier, and substrate materials, an extrinsic effect resulting from conditions within the pressure cell or a combination of the two. However, the presence of nonhydrostatic pressure components, regardless of their origin, will not affect the validity of the band-offset determinations. The only experimental requirement is that the transitions show a linear shift with pressure allowing, where necessary, an accurate extrapolation of their ambient pressure values and hence allowing a reliable determination of the ambient pressure band

offsets. Within our experimental accuracy all the transitions satisfy this requirement of a linear pressure coefficient.

IV. DISCUSSION OF RESULTS

The absolute conduction-band offsets for the SQW and MQW are $\Delta E_c = (260 \pm 19)$ and (175 ± 23) meV, respectively, or, expressed as fractions of the heavy-hole band-gap discontinuity, $\Delta E_c = (0.79 \pm 0.07)\Delta E_G^{\mathrm{HH}}$ and $(0.74 \pm 0.10)\Delta E_G^{\mathrm{HH}}$. These latter values are slightly larger than those obtained for unstrained wells where, using a similar pressure method, we have obtained values of $\Delta E_c = (0.65 \pm 0.05)\Delta E_G$ and $(0.70 \pm 0.05)\Delta E_G$ for barrier Al compositions $y = 0.58$ and 1.0, respectively.[7,8] Other groups have determined unstrained values of $\Delta E_c = 0.75\Delta E_G$ (Ref. 32) and $0.67\Delta E_G$ (Refs. 11 and 12) for $y = 0.7$ and 1.0, respectively, using a similar pressure method and $\Delta E_c = (0.65 \pm 0.05)\Delta E_G$ (Ref. 10) and $0.67\Delta E_G$ (Ref. 9) for $y = 0.6$ and 0.7 from a theoretical modeling of PLE-measured transition energies. To the best of our knowledge the only other determination of the band offsets of tensile-strained samples gave a value of $\Delta E_c \sim 0.7\Delta E_G^{\mathrm{HH}}$, deduced from a series of samples which included the SQW of the present work.[16] This value was determined by observing the well width for which the first light- and heavy-hole states cross in energy. Because this crossing occurs for narrow well widths where the transition line widths are relatively large, the precision of this result is limited. However, its value is consistent with the present more accurate results.

There have been relatively few theoretical calculations of the $Ga_xIn_{1-x}P$-$(Al_yGa_{1-y})_{0.52}In_{0.48}P$ system band offsets. Although the unstrained values agree well with those predicted by recent calculations based on Van de Walle's model solid theory,[16,33] our tensile strained values are slightly larger than those expected from this model. For example, a value of $\Delta E_c = 0.61\Delta E_G^{\mathrm{HH}}$ is predicted for the SQW compared to the experimentally determined value of $\Delta E_c = (0.79 \pm 0.07)\Delta E_G^{\mathrm{HH}}$. However, the apparent experimentally measured increase in $\Delta E_c / \Delta E_G^{\mathrm{HH}}$ between the SQW and MQW is in agreement with the model solid theory which predicts an increase in this ratio with increasing barrier Al content. The model therefore appears to predict correctly some of the observed trends in the offsets but with some errors in their absolute values.

V. DETERMINATION OF THE TYPE-II TRANSITION LIFETIME

From the measured laser power density-induced blueshift of the $X_B \rightarrow \Gamma_W$ spatially indirect type-II transition, it is possible to determine an order-of-magnitude value for the spatially separated carrier density, and also to estimate the lifetime of these carriers. Using a simple electrostatic model, Langbein *et al.*[34] have shown that, with the assumption that the carrier wave functions may be approximated by sine waves, the carrier-density dependence of the blueshift (ΔE) is given by

$$\Delta E = \frac{e^2 n}{\varepsilon \varepsilon_0} d \left(\frac{1}{12} + \frac{1}{2\pi^2} \right), \tag{5}$$

where d is the period length of the structure, and n is the two-dimensional carrier density in each layer. If we assume a linear dependence of charge density upon incident laser power for low powers (i.e., that the recombination time is independent of carrier density) then, for the MQW sample, a carrier density of $\sim 3 \times 10^{11}$ cm^{-2} is deduced to account for the blueshift observed for a 5 W cm^{-2} incident power density. Because there will be a band-gap-renormalized redshift in addition to the electrostatic blueshift, this value for the photoexcited carrier density is likely to represent a lower limit to its true value. The carrier lifetime can now be found using a standard rate equation and knowledge of the incident laser power density and the sample absorption. In the absence of detailed absorption values for $Ga_xIn_{1-x}P$ and $(Al_yGa_{1-y})In_{0.52}P_{0.48}$ the room-temperature data obtained for $Ga_{0.5}In_{0.5}P$ by Goñi *et al.*[28] are used. Their absorption curves are shifted rigidly in energy to account for the different Ga and Al compositions of the layers of the present structure, and also the pressure and temperature dependence of the band gaps. With these considerations and the above values, a carrier lifetime of $\tau \sim 1.5$ μs is deduced. Given the uncertainties in the calculation of this quantity, it should be considered at best an order-of-magnitude estimation.

The value of ~ 1.5 μs for the carrier lifetime is considerably longer than the recombination time expected for a direct real and k-space transition for which a value of ~ 1 ns is typical. The carrier lifetime is composed of two contributions, the radiative τ_R and nonradiative τ_{NR} lifetimes, through the relationship $\tau^{-1} = \tau_R^{-1} + \tau_{\mathrm{NR}}^{-1}$. Hence, given the experimentally determined value of $\tau \sim 1.5$ μs, τ_R must have a value in excess of ~ 1 μs. This large value for τ_R is consistent with that expected for a system with spatially separated carriers. Skolnick *et al.*[35] directly measured the carrier lifetime of a type-II GaAs-AlAs superlattice as a function of applied hydrostatic pressure. This increased from 0.4 to 12 μs, the variation being explained in terms of mixing between the Γ and X electron states which decreases as their energy separation is increased by the applied pressure. The present value for τ_R is consistent with these values, although the uncertainties connected with its determination makes a quantitative measurement of any variation with pressure difficult.

VI. CONCLUSIONS

The hydrostatic pressure technique has been used to deduce the band offsets of two tensile strained $Ga_xIn_{1-x}P$-$(Al_yGa_{1-y})_{0.52}In_{0.48}P$ quantum well structures. The majority of the total band-gap discontinuity is determined to be in the conduction band, a result similar to that obtained for unstrained structures. Our results indicate that the valence-band well is relatively shallow for both unstrained and tensile-strained $Ga_xIn_{1-x}P$-$(Al_yGa_{1-y})_{0.52}In_{0.48}P$ heterostructures. Hence, hole leakage by thermal emission may be an important factor limiting the performance of electro-optical devices based on this material

system. At high pressures the quantum wells become type II, and the observed indirect real and k-space transition shows a strong blueshift with increasing incident laser power density. An analysis of this blueshift allows both the photoexcited carrier density and the lifetime of the spatially separated carriers to be determined.

ACKNOWLEDGMENTS

We wish to thank the staff of Epitaxial Products International (Cardiff, United Kingdom) for the supply of the SQW, sample and the Engineering and Physical Sciences Research Council (United Kingdom) for financial support (Grant No. GR/H70270).

[1] C. P. Kuo, R. M. Fletcher, T. D. Osentowski, M. C. Lardizabal, M. G. Crawford, and V. M. Robbins, Appl. Phys. Lett. **57**, 2937 (1990).

[2] S. S. Ou, J. J. Yang, R. J. Fu, and C. J. Hwang, Appl. Phys. Lett. **61**, 892 (1992).

[3] J. A. Lott and R. P. Schneider, Jr., Electron. Lett. **29**, 830 (1993).

[4] A. R. Adams, Electron. Lett. **22**, 249 (1986).

[5] E. P. O'Reilly, G. Jones, A. Ghiti, and A. R. Adams, Electron. Lett. **27**, 1417 (1991).

[6] P. J. A. Thijs, *Digest of the 13th IEEE International Semiconductor Laser Conference* (IEEE, Takamatsu, Japan, 1992), Vol. A1, p. 2.

[7] O. P. Kowalski, J. W. Cockburn, D. J. Mowbray, M. S. Skolnick, R. Teissier, and M. Hopkinson, Appl. Phys. Lett. **66**, 619 (1995).

[8] J. W. Cockburn, O. P. Kowalski, D. J. Mowbray, M. S. Skolnick, R. Teissier, and M. Hopkinson, *Proceedings of the 22nd International Conference on the Physics of Semiconductors*, edited by D. J. Lockwood (World Scientific, Singapore, 1995), p. 747.

[9] M. D. Dawson and G. Duggan, Phys. Rev. B **47**, 12 598 (1993).

[10] C. T. H. F. Liedenbaum, A. Valster, A. L. G. H. Severens, and G. 't Hooft, Appl. Phys. Lett. **57**, 2698 (1990).

[11] D. Patel, M. J. Hafich, G. Y. Robinson, and C. S. Menoni, Phys. Rev. B **48**, 18 031 (1993).

[12] M. D. Dawson, S. P. Najda, A. H. Kean, G. Duggan, D. J. Mowbray, O. P. Kowalski, M. S. Skolnick, and M. Hopkinson, Phys. Rev. B **50**, 11 190 (1994).

[13] A. D. Prins, J. L. Sly, A. T. Meney, D. J. Dunstan, E. P. O'Reilly, A. R. Adams, and A. Valster, in *Proceedings of the 22nd International Conference on the Physics of Semiconductors* (Ref. 8), p. 719.

[14] M. D. Dawson and G. Duggan, Appl. Phys. Lett. **64**, 892 (1994).

[15] R. P. Schneider, Jr., R. P. Bryan, E. D. Jones, and J. A. Lott, Appl. Phys. Lett. **63**, 1240 (1993).

[16] M. D. Dawson, G. Duggan, and D. J. Arent, Phys. Rev. B **51**, 17 660 (1995).

[17] U. Venkateswaran, M. Chandrasekhar, H. R. Chandrasekhar, B. A. Vojak, F. A. Chambers, and J. M. Meese, Phys. Rev. B **33**, 8416 (1986).

[18] A. Gomyo, T. Suzuki, and S. Iijima, Phys. Rev. Lett. **60**, 2645 (1988).

[19] D. J. Dunstan and W. Scherrer, Rev. Sci. Instrum. **59**, 627 (1988).

[20] D. J. Mowbray, O. P. Kowalski, M. S. Skolnick, M. Hopkinson, and J. P. R. David, Superlatt. Microstruct. **15**, 313 (1994).

[21] D. J. Mowbray, O. P. Kowalski, M. Hopkinson, M. S. Skolnick, and J. P. R. David, Appl. Phys. Lett. **65**, 213 (1994).

[22] S. P. Najda, A. H. Kean, M. D. Dawson, and G. Duggan, J. Appl. Phys. **77**, 3412 (1995).

[23] R. Binder, I. Galbraith, and S. W. Koch, Phys. Rev. B **44**, 3031 (1991).

[24] J. Chen, D. Patel, J. R. Stiles, I. L. Spain, M. J. Hafich, and G. Y. Robinson, Solid State Commun. **75**, 693 (1990).

[25] R. G. Humphreys, U. Rössler, and M. Cardona, Phys. Rev. B **18**, 5590 (1978).

[26] G. Duggan and H. I. Ralph, Phys. Rev. B **35**, 4152 (1987).

[27] M. Chandrasekhar and F. H. Pollak, Phys. Rev. B **15**, 2127 (1977).

[28] A. R. Goñi, K. Syassen, K. Strössner, and M. Cardona, Phys. Rev. B **39**, 3178 (1989).

[29] R. J. Nelson and N. Holonyak, Jr., J. Phys. Chem. Solids **37**, 629 (1976).

[30] J. W. Cockburn, D. W. Peggs, O. P. Kowalski, D. J. Mowbray, M. S. Skolnick, and M. Hopkinson (unpublished).

[31] The higher Al composition of the SQW barriers raise the barrier X state by ~ 5 meV, but this effect is outweighed by the smaller strain of the SQW which increases the lowest well X state by ~ 18 meV.

[32] This value is obtained using the value for the valence-band offset determined in Ref. 13, and recently published data for the compositional dependence of the direct band gap of $(Al_yGa_{1-y})_{0.52}In_{0.48}P$ (Ref. 21).

[33] C. G. Van de Walle, Phys. Rev. B **39**, 1871 (1989).

[34] W. Langbein, S. Hallstein, H. Kalt, R. Nötzel, and K. Ploog, Phys. Rev. B **51**, 1946 (1995).

[35] M. S. Skolnick, G. W. Smith, I. L. Spain, C. R. Whitehouse, D. C. Herbert, D. M. Whittaker, and L. J. Reed, Phys. Rev. B **39**, 11 191 (1989).